

Catalysis Science & Technology

Accepted Manuscript



This is an *Accepted Manuscript*, which has been through the Royal Society of Chemistry peer review process and has been accepted for publication.

Accepted Manuscripts are published online shortly after acceptance, before technical editing, formatting and proof reading. Using this free service, authors can make their results available to the community, in citable form, before we publish the edited article. We will replace this *Accepted Manuscript* with the edited and formatted *Advance Article* as soon as it is available.

You can find more information about *Accepted Manuscripts* in the [Information for Authors](#).

Please note that technical editing may introduce minor changes to the text and/or graphics, which may alter content. The journal's standard [Terms & Conditions](#) and the [Ethical guidelines](#) still apply. In no event shall the Royal Society of Chemistry be held responsible for any errors or omissions in this *Accepted Manuscript* or any consequences arising from the use of any information it contains.

Synthesis of novel MgAl layered double oxides grafted TiO₂ cuboids and their photocatalytic activity on CO₂ reduction with water vapor

Cunyu Zhao^a, Lianjun Liu^a, Guiying Rao^a, Huilei Zhao^b, Luhui Wang^c, Jinye Xu^a,
Ying Li^{b*}

^a University of Wisconsin-Milwaukee, Mechanical Engineering Department, Milwaukee, WI 53211, USA

^b Texas A&M University, Department of Mechanical Engineering, College Station, TX 77843, USA

^c Zhejiang Ocean University, Chemical Engineering Department, Zhejiang, P.R. China

*Corresponding Author:

Prof. Ying Li

Tel: 1-979-882-4465

Fax: 1-979-845-3081

Email: yingli@tamu.edu

Abstract

A series of magnesium/aluminum (MgAl) layered double oxides (LDOs) grafted TiO₂ cuboids (MgAl-LDO/TiO₂) with various molar ratios of (Mg+Al) to Ti were synthesized by a combination of hydrothermal and coprecipitation method, in which the growth of MgAl-LDO platelets were controlled. The MgAl-LDO/TiO₂ composite materials were applied to photocatalytic CO₂ reduction with water vapor under UV light irradiation in a continuous-flow reactor. CO was found to be the main product from CO₂. At near room temperature (e.g., 50 °C), MgAl-LDO/TiO₂ did not significantly enhance CO₂ reduction compared with pure TiO₂ cuboids. At a moderately elevated reaction temperature (e.g., 150 °C), the MgAl-LDO/TiO₂ sample with an optimum 10 wt.% MgAl-LDO loading demonstrated five times higher CO₂ reduction activity than bare TiO₂ cuboids. The photo-induced electrons on TiO₂ may migrate to the MgAl-LDO/TiO₂ interfacial sites to promote CO₂ reduction. Findings in this work may lead to a new area of hybrid adsorbent/photocatalyst material that is capable of sequential CO₂ capture and photocatalytic conversion.

Keywords

Photocatalysis, CO₂ reduction, TiO₂, Hybrid materials, Layered double oxides (LDOs)

1. Introduction

Emissions of carbon dioxide (CO₂) from the consumption of fossil fuels are one of the main causes to the global climate change. Photocatalytic reduction of CO₂ with water under sunlight has been considered as a promising way to lower CO₂ level in the atmosphere and meanwhile produce alternative fuels such as carbon monoxide (CO), methane (CH₄) and methanol.^{1, 2} Among the various photocatalysts materials, TiO₂ is widely studied due to its suitable band positions, environmentally benign nature, low cost and easy availability.³⁻⁶ However, photocatalytic CO₂ reduction with water using TiO₂ as the photocatalyst typically has low energy conversion efficiency.^{1, 2, 7, 8} This is because of the major obstacles including the fast recombination rate of photo-generated electron-hole (e-h) pairs, the wide band gap of TiO₂ (3.2 eV for anatase), and the fast backward reactions.^{5, 9} Approaches such as loading noble metal or metal oxides and doping with non-metal elements have been applied to improve the CO₂ photoreduction activity of TiO₂.^{1, 10, 11} In addition to these well-known challenges, there are other factors that hinder the photocatalytic activity but are rarely studied in the literature, such as the weakened CO₂ adsorption on TiO₂ at the solid-gas interface in the presence of water vapor and limited desorption of reaction products or intermediates from the catalyst surface.^{12, 13} As a result, enhancing the CO₂ adsorption on the photocatalyst, a prior step to photoreduction, is important to improve the CO₂ photoreduction efficiency to hydrocarbon fuels.

Our previous studies have reported MgO-TiO₂ composites as hybrid adsorbent/photocatalyst materials for enhanced CO₂ photoreduction.^{12, 13} MgO was chosen as the CO₂ adsorbent because of its good CO₂ adsorption capability that is boosted in the presence of H₂O vapor.¹⁴⁻¹⁶ We found that MgO-TiO₂ possessed much higher activity and

more stable performance than pristine TiO₂, particularly at a medium temperature range (around 150 °C), which may be due to the easier desorption of reaction intermediates at a higher temperature and the enhanced CO₂ adsorption by MgO compared with bare TiO₂. We also reported that the concentration and dispersion of MgO on the MgO/TiO₂ composite strongly influenced the CO₂ photoreduction activity and 5% MgO was the optimum loading on TiO₂ surface. However, since both MgO and TiO₂ were in the form of nanoparticles in the MgO/TiO₂ composites, it was difficult to distinguish the two components by microscopic analysis and to correlate the catalytic activity with materials morphology or structure. In addition, MgO has been reported to have a relatively low kinetics in CO₂ adsorption at moderate temperatures (250-400 °C) possibly due to the changing of basic sites or –OH groups.^{17, 18} Hence, other medium temperature CO₂ sorbents with different morphologies and faster adsorption kinetics may be of greater interest to serve as the adsorbent component of the hybrid material for enhanced CO₂ photoreduction.

Layered double hydroxides (LDHs), also known as hydrotalcite-like compounds, and their post-calcination product, layered double oxides (LDOs) have been investigated as CO₂ sorbent.¹⁹⁻²¹ LDHs can be chemically expressed by a general formula $M_{1-x}^{2+}M_x^{3+}(OH)_2A_x \cdot nH_2O$, where M²⁺ and M³⁺ present metal ions and A stands for exchangeable anions (Cl⁻, NO₃⁻, CO₃²⁻, SO₄²⁻).²²⁻²⁵ The characteristics of LDHs provide the LDOs properties with a large number of Brønsted basic sites, and thus LDOs is considered as a promising candidate for CO₂ adsorption,²⁶ and activated MgAl-LDOs are found to have a high sorption capacity for CO₂.^{19, 21, 27} It is reported that MgAl-LDOs can capture much more CO₂ than MgO at the medium temperature range 150-450 °C.^{28, 29} Hence, MgAl-LDOs could be a good candidate

in replacement of MgO to combine with TiO₂ photocatalyst to improve CO₂ photoreduction operated at a medium temperature (~150 °C).

The objective of this work is to design a novel hybrid adsorbent/photocatalyst material by grafting MgAl-LDOs (as the CO₂ adsorbent component) onto the surface of micrometer size TiO₂ cuboids (as the photocatalyst component) and to investigate the catalytic activity of CO₂ photoreduction in correlation with the materials properties. To obtain such a hybrid material structure, it is desirable to have micrometer size TiO₂ for MgAl-LDOs to be grafted on because MgAl-LDOs are reported to be micrometer or sub-micrometer size platelets. The platelet-shape MgAl-LDOs can be distinct from the micrometer-size TiO₂ cuboids, and thus, the morphology and concentration of the two components can be easily manipulated.

2. Experimental

2.1. Synthesis of MgAl-LDO grafted TiO₂ cuboids

The MgAl-LDH grafted TiO₂ cuboids were synthesized by a two-step process that has not been reported before. In the first step hydrogenated titanate (H₂Ti₃O₇) nanobelts were produced and in the second step, MgAl-LDH was formed by coprecipitation with the H₂Ti₃O₇ nanobelts that were transformed into a cuboid shape along the coprecipitation process. H₂Ti₃O₇ nanobelts (micrometer in length) were prepared via a hydrothermal method that has been widely reported in the literature.³⁰⁻³² Typically, 1.0 g TiO₂ (Aeroxide P90) was dispersed in 60 ml 10 M NaOH aqueous solution with 1:1 H₂O/ethanol volume ratio. The solution was kept stirring for 30 min and then transferred to a Teflon-lined autoclave. The sodium titanate obtained after 16 h hydrothermal at 180 °C was washed with 0.1 M HCl

aqueous solution until pH 3~4 and then washed with deionized (DI) water until pH 7, forming $\text{H}_2\text{Ti}_3\text{O}_7$ nanobelts.

In the second step, the MgAl-LDH grafted TiO_2 cuboids were prepared by a coprecipitation method. The as-prepared $\text{H}_2\text{Ti}_3\text{O}_7$ nanobelts were re-dispersed in 30 ml 3.0 M urea solution to form solution A. $\text{Mg}(\text{NO}_3)_2 \cdot 6\text{H}_2\text{O}$ and $\text{Al}(\text{NO}_3)_3 \cdot 9\text{H}_2\text{O}$ were dissolved in 30 ml DI water with $[\text{Mg}^{2+}] + [\text{Al}^{3+}] = 0.15 \text{ M}$, $n(\text{Mg})/n(\text{Al}) = 2:1$ to obtain solution B. Solution B was dropwise added into solution A under stirring. The mixture was transferred to a round bottom flask in an oil bath. The flask was equipped with a water condenser with cooling water. The temperature for the mixture was set to be $\sim 95 \text{ }^\circ\text{C}$ and was kept under continuous magnetic stirring for 12 h. The obtained precipitate was washed with DI water until pH 7 and vacuum dried at $80 \text{ }^\circ\text{C}$ overnight to form MgAl-LDH grafted TiO_2 . Finally, the powder was calcined at $400 \text{ }^\circ\text{C}$ for 3 hours to form MgAl-LDO grafted TiO_2 . To find the optimum MgAl-LDO concentration in the composites to obtain the best photocatalytic CO_2 reduction activity, the samples with different mass ratio of MgAl-LDO to TiO_2 were prepared. The samples were denoted as x%MgAl-LDO/ TiO_2 , in which x represents the measured weight percentage of MgAl-LDO in the sample. Pure TiO_2 cuboids was also synthesized as the control.

2.2. Materials Characterization

The crystal structures of the MgAl-LDO/ TiO_2 samples were identified by X-ray diffraction (XRD, Scintag XDS 2000) using $\text{Cu K}\alpha$ irradiation at 45 kV, and a diffracted beam monochromator at 40 mA. The optical properties were examined by UV-vis diffuse reflectance spectroscopy using a UV-vis spectrometer (Ocean Optics) with BaSO_4 as the background. Scanning electron microscopy (SEM) (Hitachi S4800) was used to investigate

the catalyst morphology. The dispersion of elements (Mg, Al, Ti, O) on MgAl-LDO/TiO₂ was analyzed by X-ray elemental mapping. The real concentration of MgAl-LDO in the sample was calculated by the difference of the weight of MgAl-LDO/TiO₂ before and after 1 M HCl solution washing and drying.

The Brunauer-Emmett-Teller (BET) specific surface area of the composites was measured by nitrogen adsorption at 77 K on a surface area and porosity analyzer (Micrometrics ASAP 2020). Before each adsorption measurement, approximate 0.10 g sample was degassed at 180 °C for 6 hours. The BET surface area was determined by a multipoint BET method using the adsorption data in a relative pressure (P/P_0) range 0.05-0.3. The thermal stability of the catalyst materials was carried out on a thermogravimetric analyzer (TGA-DAT-2960 SDT) at a heating rate of 20 °C min⁻¹ from 25 to 700 °C in air.

2.3. Measurement of CO₂ photoreduction activity

The photocatalytic reduction of CO₂ with H₂O vapor was conducted using a home-made quartz tube photoreactor operating in a continuous flow mode, as shown in Figure S1. For each test, 100 mg catalyst was used and evenly dispersed onto a rectangular glass-fiber filter that was placed alongside the wall of the quartz tube and facing the UV light illumination. The catalyst loading process is also shown in Figure S1. Cylinder gas CO₂ (99.999%, Praxair) continuously passed through a DI water bubbler to bring a gas mixture of CO₂ + H₂O (with 2.3 vol.% H₂O) into the photoreactor. A high gas flow rate was used initially to purge out air inside the reactor for 2 h, which in the meantime ensured CO₂ adsorption reaching equilibrium on the catalyst surface. Then the flow rate was lowered and maintained at 2.0 sccm during photoreaction. A 100 W mercury vapor lamp or a 450 W Xe

lamp with a 400 nm UV cut-off filter was used as the UV-vis light and visible light source, respectively, and the light spectra are shown in Figure S2. For the mercury vapor lamp, the light intensity was measured to be about 10 mW cm^{-2} in the UV region ($\lambda < 390 \text{ nm}$, centered at 365 nm). As a reference, the UV intensity in the sunlight (AM1.5G) is around 5 mW cm^{-2} . Thus, the UV intensity from the mercury vapor lamp applied in this study was equivalent to approximately 2 suns. For the Xe lamp with UV filter, the light intensity in the visible region (400 – 700 nm) was about 84 mW cm^{-2} , again close to 2-sun condition. To reach and maintain a reaction temperature at $150 \text{ }^\circ\text{C}$, the optimum temperature found in our previous work for MgO–TiO₂ catalysts,¹³ a 250 W infrared lamp was used to heat up the photoreactor and the temperature can be adjusted by varying the distance between the IR lamp and the reactor. The gaseous products in the reactor effluent were continuously analyzed at a 15 min interval using a gas chromatograph (GC, Agilent 7890A) equipped with an automated gas valve and a thermal conductivity detector (TCD) and flame ionization detector (FID).

3. Results and Discussion

3.1. Crystal structure of MgAl-LDO/TiO₂

Figure 1 shows the XRD patterns for MgAl-LDH, MgAl-LDO, 10%MgAl-LDH/TiO₂, 10%MgAl-LDO/TiO₂ and TiO₂ cuboids samples. The diffraction peaks in both MgAl-LDH and 10%MgAl-LDH/TiO₂ patterns were indexed to MgAl-LDH^{19, 23, 33} and weaker peaks were observed for the 10%MgAl-LDH/TiO₂ sample compared with MgAl-LDH. No TiO₂ characteristic peaks were observed for 10%MgAl-LDH/TiO₂ indicating that TiO₂ crystal phase was not formed without calcination. For TiO₂ cuboids, all the diffraction peaks were attributed to the anatase phase (JCPDS No. 21-1272).^{2, 7, 8} For the MgAl-LDO sample, all the

diffraction peaks were indexed to MgO.^{12, 19, 34} For the 10%MgAl-LDO/TiO₂ samples, only TiO₂ anatase diffraction peaks are observed, and no MgO diffraction peaks are seen. The Scherrer equation was applied to calculate the crystallite size of TiO₂. The diffraction peaks of TiO₂ anatase in 10%MgAl-LDO/TiO₂ composites are narrowed compared with TiO₂ cuboids, suggesting larger crystallite size of TiO₂ due to MgAl-LDO addition. The average crystallite size of TiO₂ anatase in TiO₂ cuboids was 15 nm. By comparison, the average crystallite sizes of TiO₂ anatase in 10%MgAl-LDO/TiO₂ composites was 32 nm. A possible reason is the addition of Mg(NO₃)₂ and Al(NO₃)₃ consumes urea during the second step of material synthesis and help preserve part of the H₂Ti₃O₇ nanobelts that are later transformed to crystalline TiO₂ anatase.³²

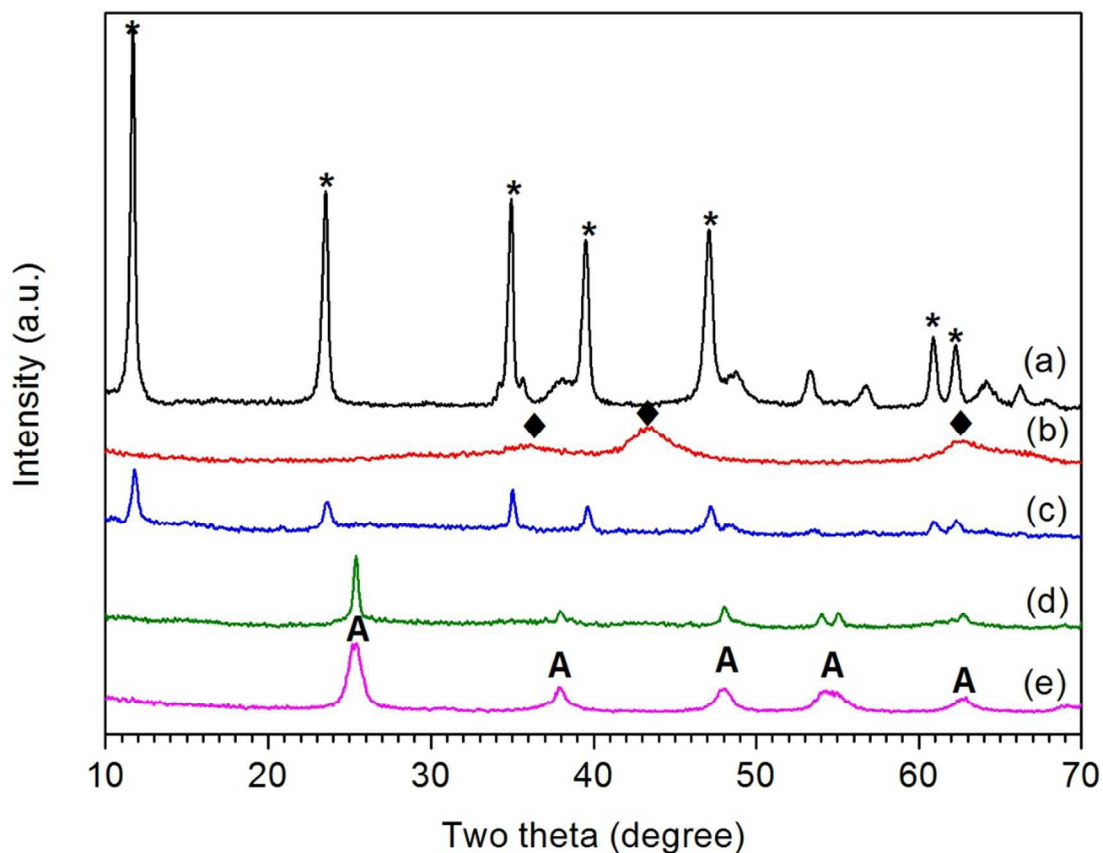


Figure 1. XRD patterns of samples: (a) MgAl-LDH; (b) MgAl-LDO; (c) 10%MgAl-LDH/TiO₂; (d) 10%MgAl-LDO/TiO₂ and (e) TiO₂ cuboids (* represents MgAl-LDH characteristic peaks, A represents TiO₂ anatase, and ◆ represents MgO characteristic peaks)

3.2. Morphology, textural structure and optical property of MgAl-LDO/TiO₂

Figure 2 shows the SEM images of H₂Ti₃O₇ titanate nanowires (precursor to TiO₂ cuboids), MgAl-LDOs and TiO₂ cuboids. MgAl-LDOs consists of platelets around 2 μm in size. The length of the TiO₂ cuboids is in micrometer size range with a high aspect ratio. The length of TiO₂ cuboids pretty much agrees with that of the titanate nanowires, suggesting that the cuboids are indeed transformed from nanowires during the second step of materials synthesis.

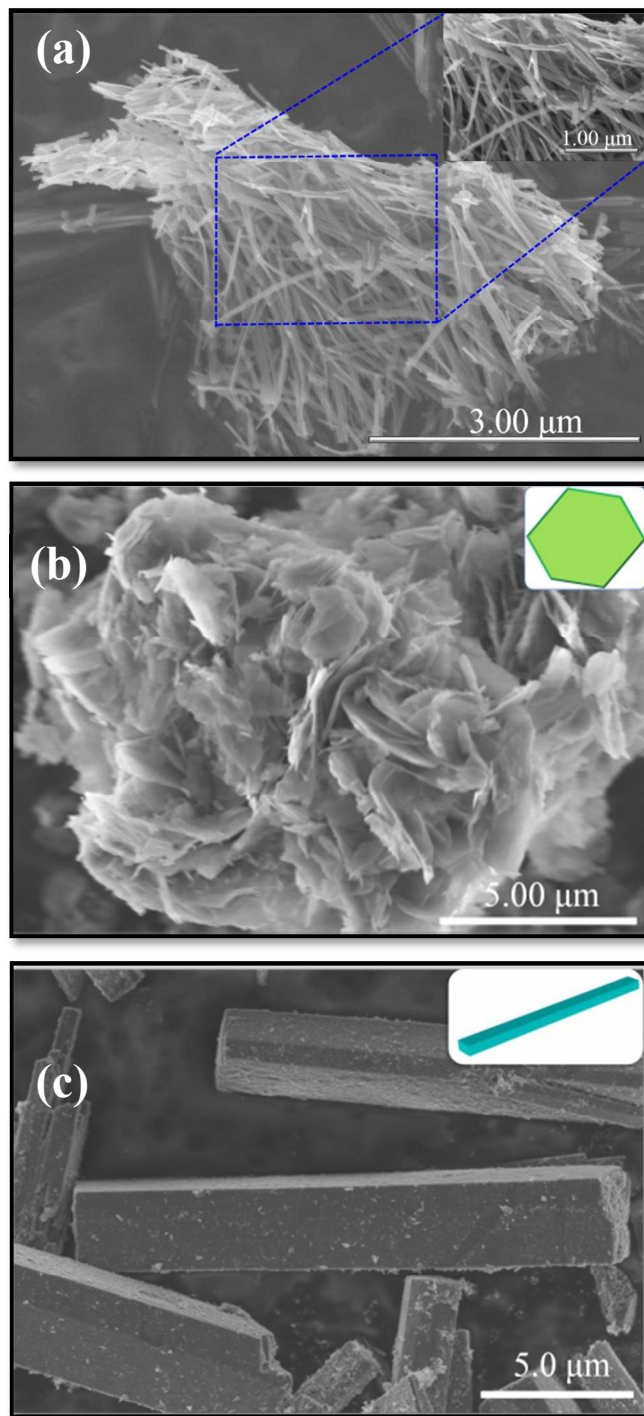


Figure 2. SEM images of (a) $\text{H}_2\text{Ti}_3\text{O}_7$ titanates, (b) MgAl-LDOs and (c) TiO_2 cuboids

Table 1. Textural properties of TiO₂, MgAl-LDO and MgAl-LDO/TiO₂ samples

Sample	BET Specific Surface Area (m ² /g)	Pore Volume (cm ³ /g)	Pore Size (nm)
TiO ₂ cuboids	109	0.48	16
10% MgAl-LDO/TiO ₂	175	0.39	9
MgAl-LDO	180	0.28	8

The textural properties are characterized by BET analysis and the results are summarized in Table 1. Bare TiO₂ cuboids displayed a specific surface area of 109 m²/g, and a pore volume of 0.48 cm³/g, where the pores are probably attributed to inter-nanoparticle spacing. The MgAl-LDO had a specific surface area of 180 m²/g, greater than that of TiO₂ cuboids, possibly due to the smaller interplanar spacing between the layered oxides, which is also reflected by the smaller pore size. Notably, the 10% MgAl-LDO/TiO₂ sample possessed a high specific surface area (175 m²/g) close to the bare MgAl-LDO, although the concentration of MgAl-LDO was not high. This indicates certain interaction between the MgAl-LDH nanoflakes and TiO₂ nanoparticles during the formation of the hybrid material.

The thermogravimetric analysis (TGA) result of the 10%MgAl-LDH/TiO₂ sample is given in Figure S3, which shows two main steps of weight loss which are in consistency with the literature.²² The adsorbed water in LDH was released at a relatively low temperature to 200 °C where mostly in the form of interlamellar water. Carbonate ions of the LDH sample were decomposed at higher temperatures from 200 to 500 °C in parallel with the water loss. The weight loss almost ceased at above 500 °C indicating the complete of decarbonation process, i.e., LDH was fully converted to LDO.

Figure 3 shows the SEM images of MgAl-LDO/TiO₂ samples with different compositions. The lower magnification SEM images in Figures 3-a,c,e show that the three samples were composed of MgAl-LDOs grafted on micrometer size TiO₂ cuboids. The platelet shape of MgAl-LDOs on the composites after calcination was almost the same as the as-prepared uncalcined composites MgAl-LDHs (SEM images not shown here). In most of the literature reports, the morphology of MgAl-LDHs platelets cannot be maintained after calcination.^{25, 35} The successful grafting of MgAl-LDO platelets on micrometer-size TiO₂ cuboids in this work demonstrates a novel approach in synthesizing such composite materials with desired morphology. The higher magnification SEM images in Figures 3-b,d,f show both the size and the coverage of MgAl-LDO platelets grafted on TiO₂ cuboids increased as the MgAl-LDO loading increased.

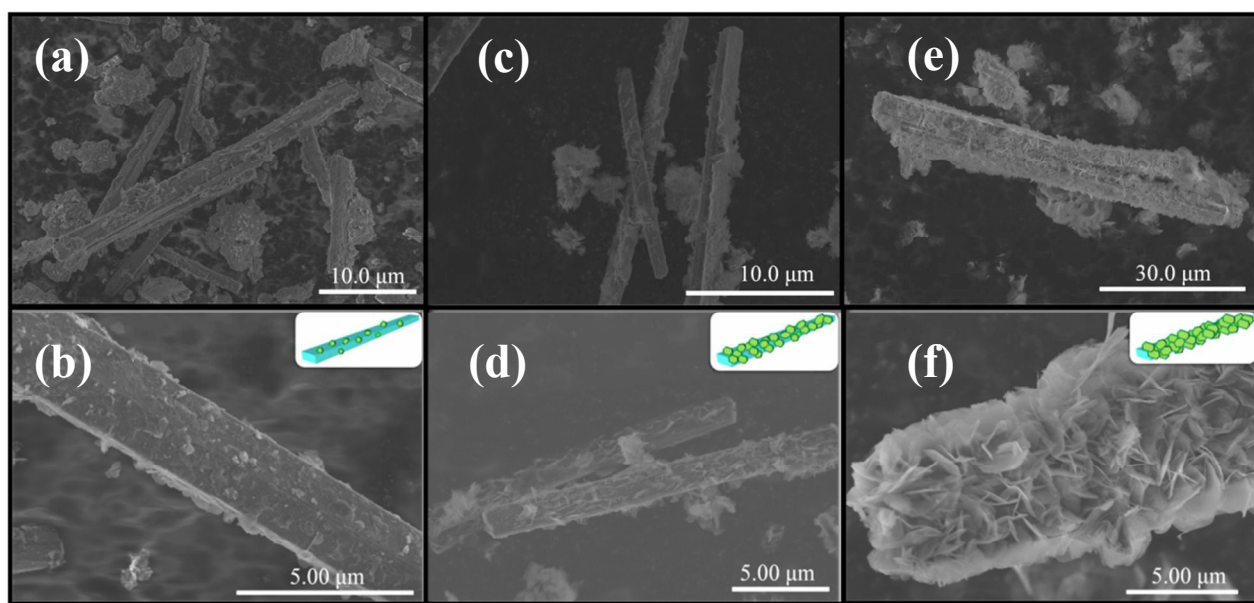


Figure 3. SEM images of the MgAl-LDO/TiO₂ composites: (a,b) 8% MgAl-LDO/TiO₂, (c,d), 10% MgAl-LDO/TiO₂, and (e,f) 12% MgAl-LDO/TiO₂.

The distributions of Mg, Al, Ti and O elements in the MgAl-LDO/TiO₂ composites were analyzed by X-ray elemental mapping, and the results are shown in Figure 4. The elemental mapping images demonstrated that the cuboids skeleton were mainly composed of Ti element and the grafted platelets were composed of Mg and Al elements that were evenly distributed on the cuboids surface. The O element is distributed on both the cuboids and the platelets, agreeing with the composition of mixed oxides for this composite material.

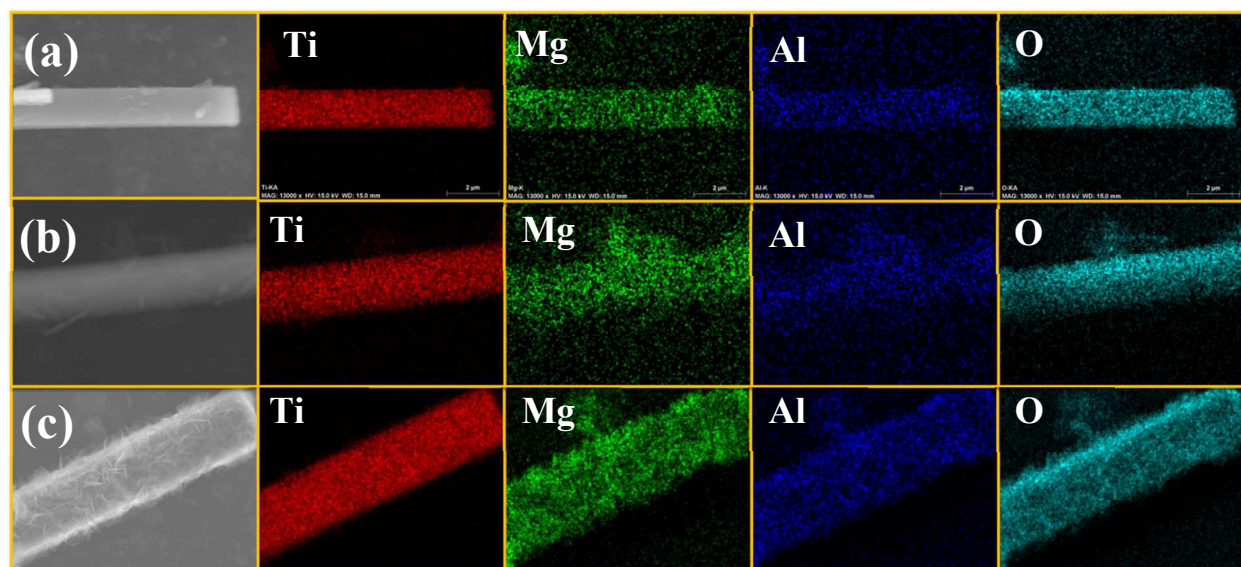


Figure 4. X-ray elemental mapping images of the MgAl-LDO/TiO₂ composites: (a) 8%MgAl-LDO/TiO₂, (b) 10%MgAl-LDO/TiO₂, and (c) 12%MgAl-LDO/TiO₂.

Diffuse reflectance UV-vis spectra were recorded to investigate the influence of MgAl-LDO on the optical property of TiO₂, and the plots of Kubelka-Munk function were made to determine the band gap values, as shown in Figure 5. The absorption edge of the TiO₂ is around 390 nm, corresponding to a band gap of about 3.2 eV, which agrees with most reported literature data on the band gap of TiO₂ anatase. The MgAl-LDO alone shows no light adsorption in the wavelength range measured. The incorporation of MgAl-LDOs on

TiO₂ cuboids leads to a slight blue-shift in the adsorption edge and a reduced absorption in the UV region, probably due to the increased surface roughness resulting in more reflection.

To further confirm possible structural changes, UV/Vis adsorption spectra of H₂Ti₃O₇ and 10%MgAl-LDH/TiO₂ were recorded and shown in Figure S4. By comparing TiO₂ cuboids with H₂Ti₃O₇, TiO₂ cuboids has a red-shift in the absorption edge, which indicates compositional changes due to the calcination of H₂Ti₃O₇. By comparing 10%MgAl-LDH/TiO₂ with 10%MgAl-LDO/TiO₂, difference in the absorption shift is also observed due to the conversion of LDH to LDO. By comparing MgAl-LDO/TiO₂ with TiO₂ cuboids, there is less absorption in the UV region for the MgAl-LDO/TiO₂, which indicates possible interaction of MgAl-LDO with TiO₂.³⁶ From the XRD results, there is no obvious change of TiO₂ diffraction peaks or appearance of new peaks, suggesting the extent of Mg atoms incorporation into the TiO₂ structure, if any, is not significant.

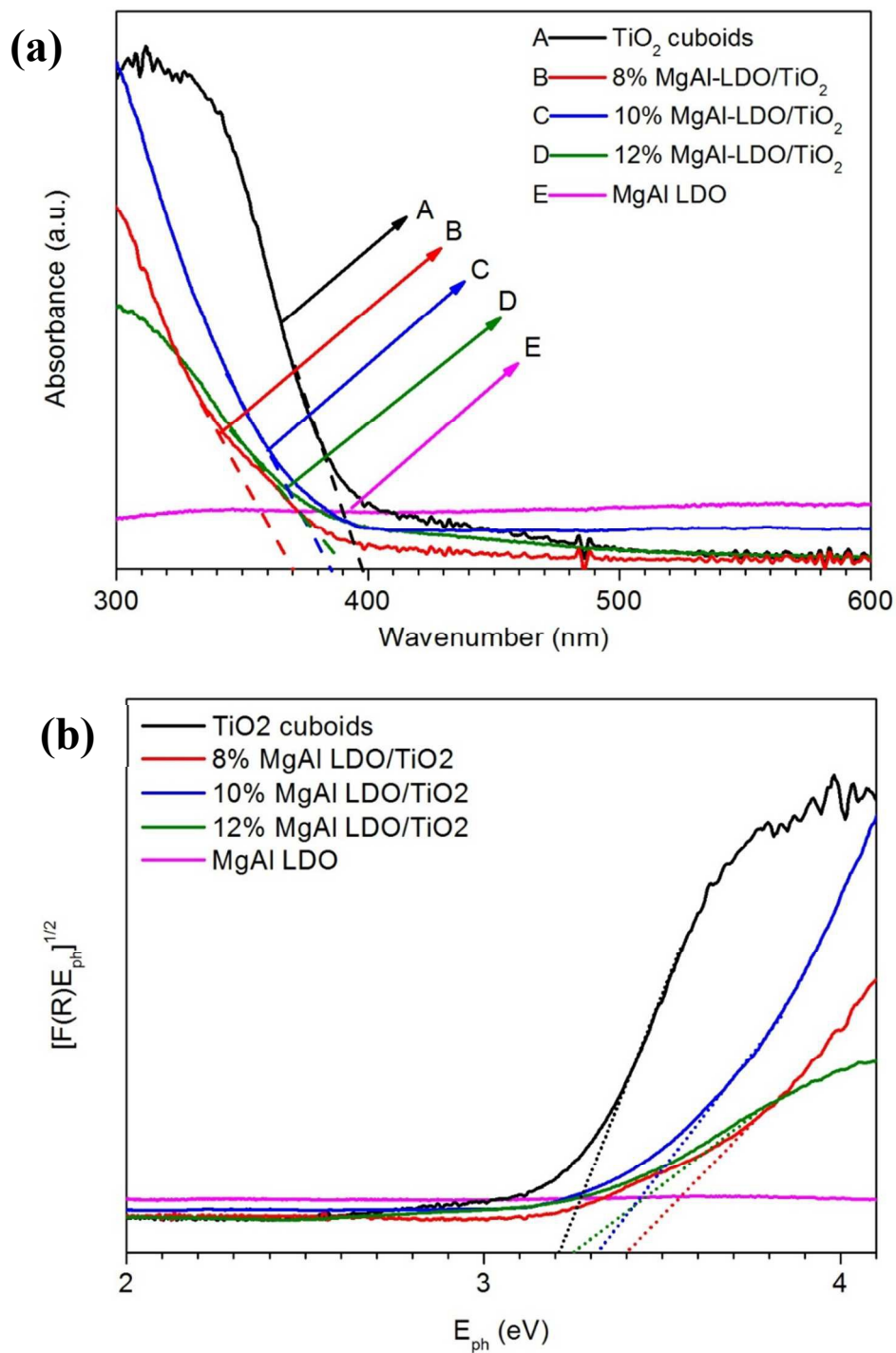


Figure 5. (a) UV-vis diffuse reflectance spectra and (b) plots of the square root of Kubelka-Munk function versus the photon energy for the catalyst materials of TiO_2 cuboids, MgAl-LDO, and MgAl-LDO/ TiO_2 composites with different MgAl-LDO concentrations.

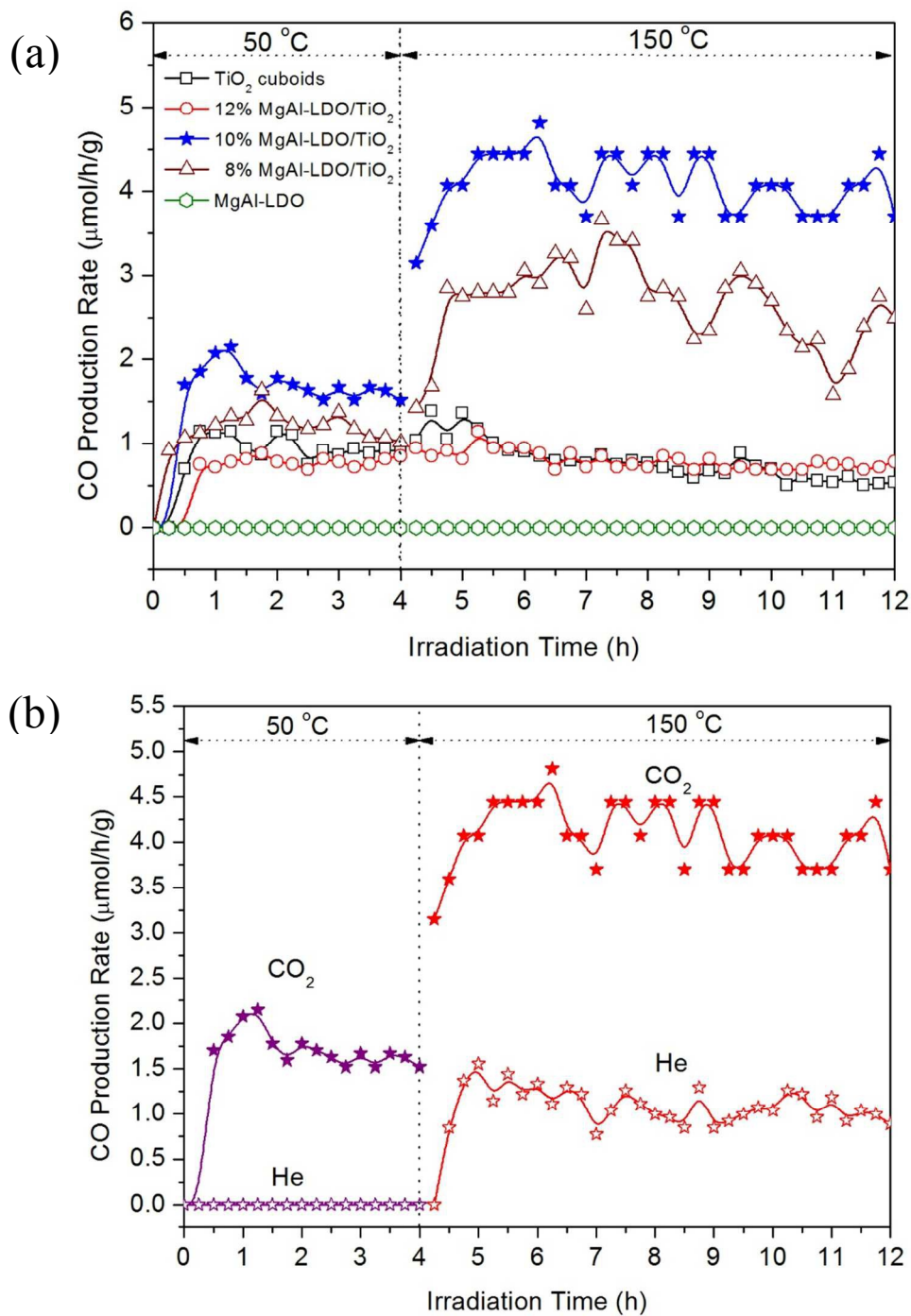
3.3. Photocatalytic activities of CO₂ reduction

Figure 6. The rate of CO production from CO₂ photoreduction under UV light irradiation at 50 °C for 4 h and subsequently at 150 °C for 8 h using (a) TiO₂ cuboids, MgAl-LDO and three MgAl-LDO/TiO₂ composites in CO₂ + H₂O vapor atmosphere, and (b) 10%MgAl-LDO/TiO₂ in He+H₂O vapor atmosphere and CO₂+ H₂O vapor atmosphere, respectively.

Photocatalytic activity tests were carried out under UV light irradiation at 50 °C for 4 h (Figure 6a) and subsequently at 150 °C for another 8 h (Figure 6b). CO was found to be the major product with a minor CH₄ concentration that was one or two orders of magnitude lower than CO. Thus, only CO production results were shown in Figure 6 to compare the activities of the different catalysts. Figure 6a shows bare TiO₂ cuboids had a CO production rate around 1.0 μmol g⁻¹ h⁻¹ at 50 °C while pure MgAl-LDO had no activity for CO production. The addition of MgAl-LDO on TiO₂ cuboids had no significant improvement for CO production rate except for the 10%MgAl-LDO/TiO₂ sample that has a doubled activity compared with bare TiO₂ cuboids. The main reason for such insignificant improvement is maybe because MgAl-LDOs has weak CO₂ adsorption at low temperatures.²⁶

For the following 8 h test under UV light at 150 °C (Figure 6b), the CO production rate of bare TiO₂ cuboids was almost the same as the first 4 hours at 50 °C. Pure MgAl-LDOs still showed no activity of CO₂ reduction. Both 8%MgAl-LDO/TiO₂ and 10%MgAl-LDO/TiO₂ exhibited an obvious enhancement in CO production, reaching an average at about 2.8 and 4.3 μmol g⁻¹ h⁻¹, respectively, compared with about 0.7 μmol g⁻¹ h⁻¹ for bare TiO₂ cuboids at 150 °C. In another word, 10%MgAl-LDO/TiO₂ was five times more active than bare TiO₂ cuboids. Moreover, the activities of both 8%MgAl-LDO/TiO₂ and 10%MgAl-LDO/TiO₂ at 150 °C were much higher than those at 50 °C. In addition, the downward trend in CO production rate for the 8%MgAl-LDO/TiO₂ sample indicates that it is inferior to the 10%MgAl-LDO/TiO₂ sample in terms of stability. Interestingly, the activity of 12%MgAl-LDO/TiO₂ did not show any enhancement compared with bare TiO₂ no matter at 50 °C or 150 °C. The above results indicate that at an optimum MgAl-LDO loading (10% in this study), the CO₂ reduction activity can be significantly increased at a higher temperature (150

°C). It also agrees with our hypothesis that the CO₂ adsorption capability of MgAl-LDOs could promote the CO₂ photoreduction capability by TiO₂. It is likely that the photo-induced electrons on TiO₂ could migrate to the adjacent CO₂ adsorption sites at the interface of TiO₂ and MgAl-LDO and thus promote CO₂ reduction. However, the exact mechanism is not clear so far and will be investigated in our future research. Too high a loading of MgAl-LDO (12% in this case) did not promote CO₂ photoreduction or may have detrimental effect, probably because of the following two reasons: (1) the MgAl-LDOs may have covered all the TiO₂ cuboids surfaces (Figure 3f) so that the contact between TiO₂ and adsorbed CO₂ is limited, and (2) the light absorption capacity is significantly reduced at a high MgAl-LDO loading (Figure 5).

The CO₂ photoreduction with H₂O by the 10% MgAl-LDO/TiO₂ sample under visible light was also carried out using a Xe lamp equipped with a 400 nm cut-off filter, and the result is shown in Figure S5. At 50 °C under visible light, the catalyst exhibited no activity and at 150 °C, the CO production rate reached around 1.0 μmol g⁻¹ h⁻¹. Apparently, the material is more active under UV than under visible light, which agrees with the band gap of the material as shown in Figure 5.

To examine the cycling capability of the catalyst, an additional experiment was conducted using 10%MgAl-LDO/TiO₂ under the mercury vapor lamp irradiation at 150 °C for two on-and-off cycles for a total period of 12 h. The results are shown in Figure S6. The CO production rate was around 4.0 μmol g⁻¹ h⁻¹ when light was on. When the light was switched off, the CO production rate decreased rapidly and became zero within one hour. Turning the light back on obviously re-activated the photoreduction and the CO production rate bounced back to 3.6 μmol g⁻¹ h⁻¹, almost the same level as in the first cycle. Switching

off the light again led to a stop in the photoreduction. This on-and-off cycling test result clearly indicates that CO production was indeed from CO₂ photoreduction with water activated by the UV light irradiation. The result that CO production rate in the 2nd cycle can be recovered to the similar level in the 1st cycle demonstrates a good cycling capability of the catalyst.

Because the MgAl-LDO may still contain a small amount carbonate species even after the calcination process, we have conducted another set of experiments to understand the possible interference of carbonate species on the catalyst to the reduction of CO₂ from the gas phase. Tests were carried out by comparing the photocatalytic activity of 10%MgAl-LDO/TiO₂ under two gas environments: (1) helium (He) + H₂O vapor and (2) CO₂+H₂O vapor, and the results are shown in Figure 6b. There was no CO production in He+H₂O atmosphere at 50 °C, but when the temperature was increased to 150 °C, CO was produced at a rate about 1.0 μmol g⁻¹ h⁻¹. This result indicates that carbonates in MgAl-LDOs were stable at low temperatures but were activated at higher temperatures and reduced to CO through photocatalytic reactions. By contrast, when CO₂ was present, the CO production rate was much higher, 1.5 μmol g⁻¹ h⁻¹ at 50 °C and 4.3 μmol g⁻¹ h⁻¹ at 150 °C. Comparison of these results suggests that carbonate residues in the MgAl-LDO/TiO₂ composites did not have significant contribution to the CO production and most of it was derived from gas-phase CO₂ reduction. To further verify the source of CO production, additional experiments were conducted to measure the photocatalytic activity of H₂Ti₃O₇ and TiO₂ cuboids in He/H₂O atmosphere, and the result is shown in Figure S7. No CO production was observed for H₂Ti₃O₇ and TiO₂ cuboids at either 50 °C or 150 °C. Only 10% MgAl-LDO/TiO₂ showed some CO production at 150 °C. This result further proved that the small amount of CO

produced in the He/H₂O atmosphere was attributed to carbonate residues in the MgAl-LDO component of the composite and not from carbon contamination of TiO₂.

On the other hand, the above interesting finding suggests that if we pre-load carbonates on the composite catalyst by capturing CO₂ first and then expose the material under UV light or sunlight, it is possible that we can convert the captured CO₂ into CO in the second step, and thus we can separate the CO₂ capture and conversion process. A benefit of doing this is to achieve separation of CO₂ conversion products (e.g., CO) from the bulk CO₂, an approach advantageous to most CO₂ photoreduction processes reported in the literature where the products are mixed with unreacted CO₂. We will conduct further research to investigate this novel idea.

4. Conclusions

This work has demonstrated the successful synthesis of novel hybrid materials, MgAl-LDOs platelets grafted on TiO₂ cuboids, with controlled mass ratio of MgAl-LDO to TiO₂. The surface coverage of MgAl-LDO on TiO₂ and the reaction temperature are two important parameters that influence the activity of CO₂ photocatalytic reduction to CO. The hybrid MgAl-LDO/TiO₂ showed five times higher CO production rate than bare TiO₂ at the optimum 10 wt.% MgAl-LDO loading and at 150 °C. The possible reason for the enhancement is that the grafted MgAl-LDOs function as CO₂ adsorbent and its CO₂ capture ability increases with increasing temperature (in the range less than 200 °C) and that the photoinduced electrons generated on TiO₂ may migrate to the interfacial sites and promote CO₂ reduction. At too high a loading of MgAl-LDO when the platelets completely cover the TiO₂ cuboids surface, the light absorption ability is impaired and the contact between TiO₂ and CO₂ is blocked, and thus no improvement

in CO₂ photoreduction is observed. The carbonate residues on the MgAl-LDO/TiO₂ have a minor contribution to the CO production under photoirradiation, which inspires a new process of sequential CO₂ capture and photocatalytic conversion to fuels using this novel hybrid material. In this case, the products can be effectively separated from unreacted CO₂. This interesting idea will be validated in our future work.

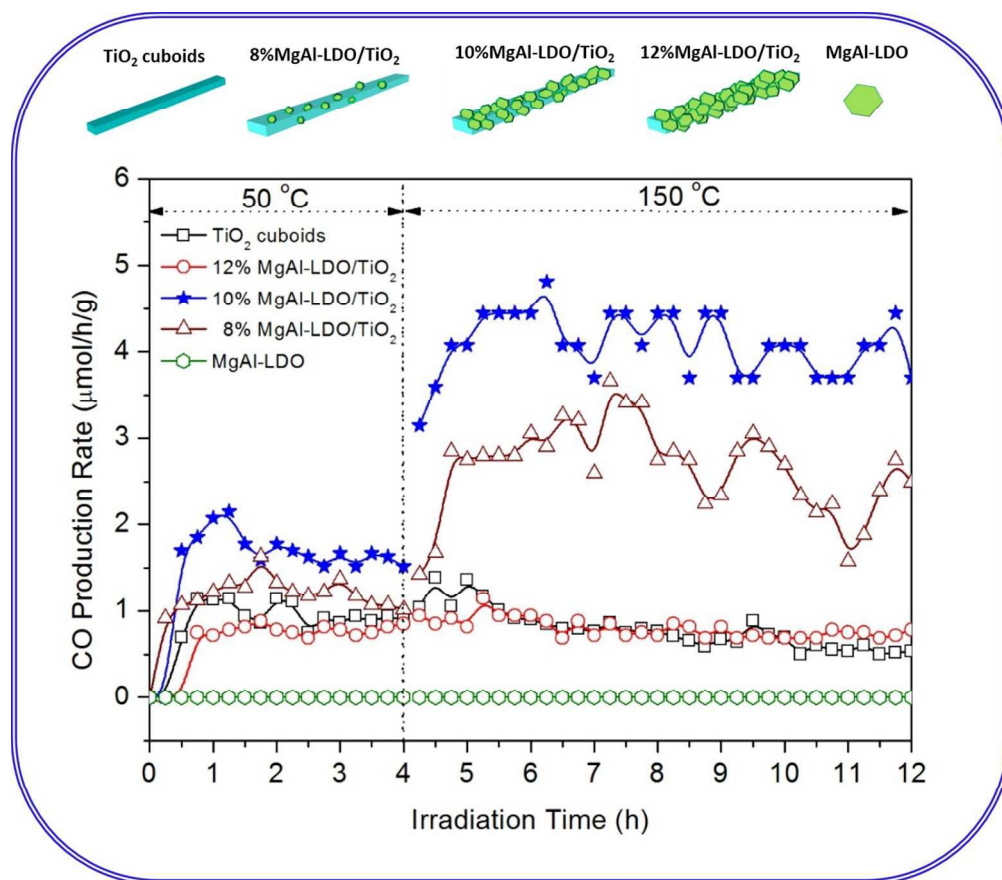
Acknowledgments

The authors acknowledge the financial support from National Science Foundation (NSF) Early Faculty CAREER Award (CBET-1254709).

References

1. C. Y. Zhao, A. Krall, H. L. Zhao, Q. Y. Zhang and Y. Li, *Int. J. Hydrogen Energy*, 2012, 37, 9967-9976.
2. L. J. Liu, D. T. Pitts, H. L. Zhao, C. Y. Zhao and Y. Li, *Appl. Catal., A*, 2013, 467, 474-482.
3. L. J. Liu, H. L. Zhao, J. M. Andino and Y. Li, *Acs Catalysis*, 2012, 2, 1817-1828.
4. Y. Li, W. N. Wang, Z. L. Zhan, M. H. Woo, C. Y. Wu and P. Biswas, *Appl. Catal., B*, 2010, 100, 386-392.
5. Q. Y. Zhang, Y. Li, E. A. Ackerman, M. Gajdardziska-Josifovska and H. L. Li, *Appl. Catal., A*, 2011, 400, 195-202.
6. C. L. Yu, Q. Z. Fan, Y. Xie, J. C. Chen, Q. Shu and J. C. Yu, *J. Hazard. Mater.*, 2012, 237, 38-45.
7. C. Y. Zhao, L. J. Liu, Q. Y. Zhang, J. Wang and Y. Li, *Catal. Sci. Technol.*, 2012, 2, 2558-2568.
8. H. L. Zhao, L. J. Liu, J. M. Andino and Y. Li, *J. Mater. Chem.A*, 2013, 1, 8209-8216.
9. I. H. Tseng, J. C. S. Wu and H. Y. Chou, *J. Catal.*, 2004, 221, 432-440.
10. R. Asahi, T. Morikawa, T. Ohwaki, K. Aoki and Y. Taga, *Science*, 2001, 293, 269-271.
11. Y. Kohno, H. Hayashi, S. Takenaka, T. Tanaka, T. Funabiki and S. Yoshida, *J. Photochem. Photobiol., A*, 1999, 126, 117-123.
12. L. J. Liu, C. Y. Zhao, H. L. Zhao, D. Pitts and Y. Li, *Chem. Commun.*, 2013, 49, 3664-3666.
13. L. Liu, C. Zhao, D. Pitts, H. Zhao and Y. Li, *Catal. Sci. Technol.*, 2014, 2014, 1539-1546.
14. Y. Kohno, H. Ishikawa, T. Tanaka, T. Funabiki and S. Yoshida, *Phys Chem Chem Phys*, 2001, 3, 1108-1113.
15. Q. Y. Li, L. L. Zong, C. Li and J. J. Yang, *Appl Surf Sci*, 2014, 314, 458-463.
16. S. J. Xie, Y. Wang, Q. H. Zhang, W. Q. Fan, W. P. Deng and Y. Wang, *Chem. Commun.*, 2013, 49, 2451-2453.
17. G. Xiao, R. Singh, A. Chaffee and P. Webley, *Int. J. Greenhouse Gas Control*, 2011, 5, 634-639.
18. A. Chakradhar and U. Burghaus, *Surf. Sci.*, 2013, 616, 171-177.
19. Y. S. Gao, Z. Zhang, J. W. Wu, X. F. Yi, A. M. Zheng, A. Umar, D. O'Hare and Q. Wang, *J. Mater. Chem.A*, 2013, 1, 12782-12790.
20. J. W. Wang, L. A. Stevens, T. C. Drage and J. Wood, *Chem. Eng. Sci.*, 2012, 68, 424-431.
21. M. Dadwhal, T. W. Kim, M. Sahimi and T. T. Tsotsis, *Ind. Eng. Chem. Res.*, 2008, 47, 6150-6157.

22. T. Bujdoso, A. Patzko, Z. Galbacs and I. Dekany, *Appl. Clay Sci.*, 2009, 44, 75-82.
23. K. Teramura, S. Iguchi, Y. Mizuno, T. Shishido and T. Tanaka, *Angew. Chem., Int. Ed.*, 2012, 51, 8008-8011.
24. M. Q. Zhao, Q. Zhang, J. Q. Huang and F. Wei, *Adv. Funct. Mater.*, 2012, 22, 675-694.
25. Y. Kuang, L. N. Zhao, S. A. Zhang, F. Z. Zhang, M. D. Dong and S. L. Xu, *Materials*, 2010, 3, 5220-5235.
26. M. K. R. Reddy, Z. P. Xu, G. Q. Lu and J. C. D. Da Costa, *Ind. Eng. Chem. Res.*, 2006, 45, 7504-7509.
27. M. Leon, E. Diaz, S. Bennici, A. Vega, S. Ordonez and A. Auroux, *Ind. Eng. Chem. Res.*, 2010, 49, 3663-3671.
28. J.-I. Yang and J.-N. Kim, *Korean J. Chem. Eng.*, 2006, 23, 77-80.
29. X. P. Wang, J. J. Yu, J. Cheng, Z. P. Hao and Z. P. Xu, *Environmental Science & Technology*, 2008, 42, 614-618.
30. Z. Yang, G. Du, Z. Guo, X. Yu, Z. Chen, T. Guo and H. Liu, *J. Mater. Chem.*, 2011, 21, 8591-8596.
31. Q. Li, J. Zhang, B. Liu, M. Li, S. Yu, L. Wang, Z. Li, D. Liu, Y. Hou, Y. Zou, B. Zou, T. Cui and G. Zou, *Cryst. Growth Des.*, 2008, 8, 1812-1814.
32. Q. Li, J. Zhang, B. Liu, M. Li, R. Liu, X. Li, H. Ma, S. Yu, L. Wang, Y. Zou, Z. Li, B. Zou, T. Cui and G. Zou, *Inorg. Chem.*, 2008, 47, 9870-9873.
33. J. Wang, D. D. Li, X. A. Yu, M. L. Zhang and X. Y. Jing, *Colloid Polym. Sci.*, 2010, 288, 1411-1418.
34. N. C. S. Selvam, R. T. Kumar, L. J. Kennedy and J. J. Vijaya, *J. Alloys Compd.*, 2011, 509, 9809-9815.
35. Y. S. Zhao, J. G. Li, F. Fang, N. K. Chu, H. Ma and X. J. Yang, *Dalton Trans.*, 2012, 41, 12175-12184.
36. Š. Paušová, J. Krýsa, J. Jirkovský, G. Mailhot and V. Prevot, *Environ Sci Pollut Res*, 2012, 19, 3709-3718.



Photocatalytic CO₂ Reduction with H₂O by Hybrid MgAl-LDO/TiO₂ Materials
217x189mm (150 x 150 DPI)